Journal of Electroceramics, 13, 41–45, 2004

Effect of Zr/Ti Ratio on Microstructure and Electrical Properties of Lead Zirconate Titanate Thin Films Derived by Pulsed Laser Deposition

ZHAN JIE WANG,[1,*] YUKI AOKI,[1] HIROYUKI KOKAWA,[1] MASAAKI ICHIKI[2] & RYUTARO MAEDA[2]

[1] *Department of Materials Processing, Graduate School of Engineering, Tohoku University, Aoba-yama 02 Sendai 980-8579, Japan*

[2] *National Institute of Advanced Industrial Science and Technology, 1-2 Namiki, Tsukuba 305-8564, Japan*

Submitted February 11, 2003; Revised November 9, 2003; Accepted January 26, 2004

Abstract. PZT films were fabricated using various targets of $Pb(Zr_xTi_{1-x})O_3$ with Zr/Ti ratios of 70/30, 58/42, 52/48, 45/55 and 30/70, and with excess PbO of 20 wt% on $Pt/Ti/SiO_2/Si(100)$ substrates. The rosette structure was observed in the films derived from the target with a Zr/Ti ratio of 70/30 and disappeared with increasing titanium composition. The observations on surface and cross-sectional microstructure were consistent with a higher perovskite nucleation for the higher Ti content films. The PZT films derived from the target with a Zr/Ti ratio of 45/55 had a polycrystalline columnar microstructure extending throughout the thickness of the film and no pyrochlore phase on the surface was observed. The PZT films derived from the target with a Zr/Ti ratio of 45/55 exhibited better electric properties than those derived from the target with a Zr/Ti ratio of 52/48.

Keywords: lead zirconate titanate, thin film, pulsed laser deposition, crystalline phases, microstructure, ferroelectric properties

1. Introduction

Lead zirconate titanate $Pb(Zr_xTi_{1-x})O_3$ (PZT) have been extensively studied because of their excellent ferroelectric, pyroelectric and piezoelectric properties. Many potential applications of PZT thin films in Micro Electro Mechanical Systems (MEMS) have been reported recently, for example, as atomic force microscopy (AFM) cantilevers [1, 2] andmicro-scanning mirror devices [3, 4]. For use in these microactuators, in order to obtain a large displacement, high-quality 3-μm-thick PZT films on electrodes/substrates are desirable [2, 5]. Many fabrication techniques, such as the sol-gel method [6], pulsed laser deposition (PLD) [7] nd sputtering [8] have been used to fabricate ferroelectric PZT thin films. PLD is a promising technique for PZT film fabrication, because it offers the advantage of a high deposition rate, which allows a thicker PZT film to be fabricated in a shorter time [7].

*To whom all correspondence should be addressed. E-mail: wangzj@argon.material.tohoku.ac.jp

In $Pb(Zr_xTi_{1-x})O_3$ bulk ceramic, the composition with $x = 0.52$ crystallizes in a two-phase system of both tetragonal and rhombohedral perovskite phases (morphotropic phase boundary). It is well known that the relative permittivity and the piezoelectric coupling factor of $Pb(Zr_xTi_{1-x})O_3$ polycrystal located at the morphotropic phase boundary $x = 0.52$ show maximum values [9]. In our previous work, we noted that the Pb/(Zr + Ti) ratio in the films fabricated from the target of $Pb(Zr_{0.52}Ti_{0.48})O_3$ with excess PbO (20 wt%) was almost equivalent to the stoichiometric amount (50/50), but the Zr/Ti ratio was about 60/40 and was higher than the amount of the morphotropic phase boundary (MPB) (52/48) [7]. It was found that the PZT films derived from the target with a Zr/Ti ratio of 45/55 exhibited better electric properties than that derived from the target with a Zr/Ti ratio of 52/48 [10]. However, the effect of Zr/Ti ratio in target on the microstructure of the films remains unknown and further investigations are required.

In this work, the PZT films were fabricated form the targets of $Pb(Zr_xTi_{1-x})O_3$ with Zr/Ti ratios of 70/30, 58/42, 52/48, 45/55 and 30/70, and with excess PbO

(20 wt%), and their microstructure and electrical properties were investigated. Based on these results, the electrical properties and microstructure of the PZT films were correlated with their composition.

2. Experimental

Substrates were prepared by sputtering 0.05 μm of titanium and 0.15 μm of Pt onto oxidized (1.8 μm of SiO_2) Si(100) substrates, and then a thin PZT template layer was deposited on Pt/Ti/SiO_2/Si(100) substrates using the sol-gel process. The template layer could lower the annealing temperature in the PLD processing, and their thickness was about 130 nm [11].

The PZT films of 0.6 μm thickness were deposited by PLD on the above-mentioned substrates. The targets used were ceramic pellets (relative density: about 85%) of $Pb(Zr_xTi_{1-x})O_3$ with Zr/Ti ratios of 70/30, 58/42, 52/48, 45/55 and 30/70 and with 20 wt% excess PbO. A KrF excimer laser (wavelength: 248 nm) was used, and the PZT thin films were deposited at room temperature. The details about the PLD system and processing parameters were reported previously [10]. After pulsed laser deposition, the PZT films were annealed at 700°C for 90 min.

The crystalline structure of the PZT films was examined using an X-ray diffractometer (XRD, Rigaku RINT2000, Cu K_α Radiation). The surface and cross-sectional morphology of the films were observed by scanning electron microscopy (FE-SEM, JSM-6500F). The microstructure of the films was observed by transmission electron microscopy (FE-TEM, HITACHI-HF2000). The Pt/Ti film was used as a bottom electrode, and an Au/Cr film (size: ϕ1.5 mm) was deposited by vacuum evaporation to form the top electrode. The P-E hysteresis loop of these films was measured using a standard ferroelectric test system (Radiant Technologies RT-60 A). The dielectric constant and dielectric loss tangent of these films were measured at 1 kHz using an impedance analyzer (Hewlett-Packard, HP4192A).

3. Results and Discussion

3.1. Crystalline Phases of the PZT Films

The XRD analysis showed that all the films consisted of mainly the perovskite phase without the pyrochlore phase. Figure 1 shows the XRD patterns of the PZT films deposited from targets with Zr/Ti ratios of 45/55 and 30/70 to give examples. The XRD patterns of the films fabricated from targets with Zr/Ti ratios of 70/30, 58/42, 52/48 are similar to that of the film fabricated from the target with Zr/Ti ratios of 45/55 (Fig. 1(a)), and showed only strong and sharp peaks of the (100), (111) and (200) planes. This means that the PZT films fabricated from targets with Zr/Ti ratios of 70/30, 58/42, 52/48 and 45/55 mainly crystallized in the rhombohedral perovskite phase. The PZT film fabricated from the target with a Zr/Ti ratio of 30/70 had the split peaks of (110) and (101), (100) and (001) planes (Fig. 1(b)), and mainly crystallized in the tetragonal perovskite phase. The lattice constant calculated from

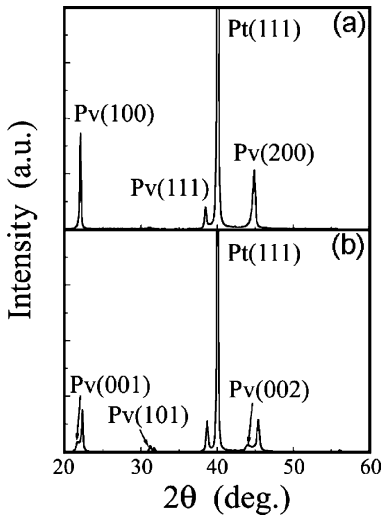

Fig. 1. XRD patterns of the films fabricated from targets with Zr/Ti ratios of (a) 45/55 and (b) 30/70. Pv: perovskite phase.

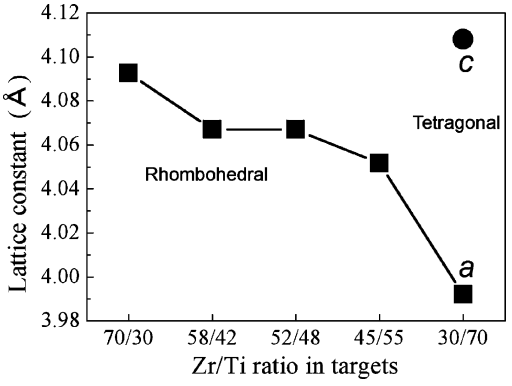

Fig. 2. Lattice constant as a function of Zr/Ti ratio in the $Pb(Zr_xTi_{1-x})O_3$ targets.

the XRD patterns of the PZT films is shown as a function of the composition in Fig. 2. The lattice constant a of the rhombohedral phase decreases with increasing titanium composition in the rhombohedral films. The lattice constants of the tetragonal perovskite phase for the film fabricated from the target with a Zr/Ti ratio of 30/70 were $a = 0.3992$ nm and $c = 0.4108$ nm, with c/a equal to 1.3. Figure 2 also shows that the Zr/Ti ratio in the films derived from the target with a Zr/Ti ratio of 45/55 is closer to the amount of the morphotropic phase boundary than the Zr/Ti ratio of 52/48.

3.2. Surface Morphology of the PZT Films

Figure 3 shows the change on the surface morphology of the PZT films as a function with Zr/Ti ratio. Round spheres ("rosettes", see Ref. 12) with diameters of 5–15 μm were observed on the film fabricated from the target with a Zr/Ti ratio of 70/30 (Fig. 3(a)). The rosette structure was also observed before and identified as the perovskite phase [12–14]. The areas of matrix between the rosettes were fine-grained pyrochlore phase, which could not be detected by XRD analyses [13, 15]. This

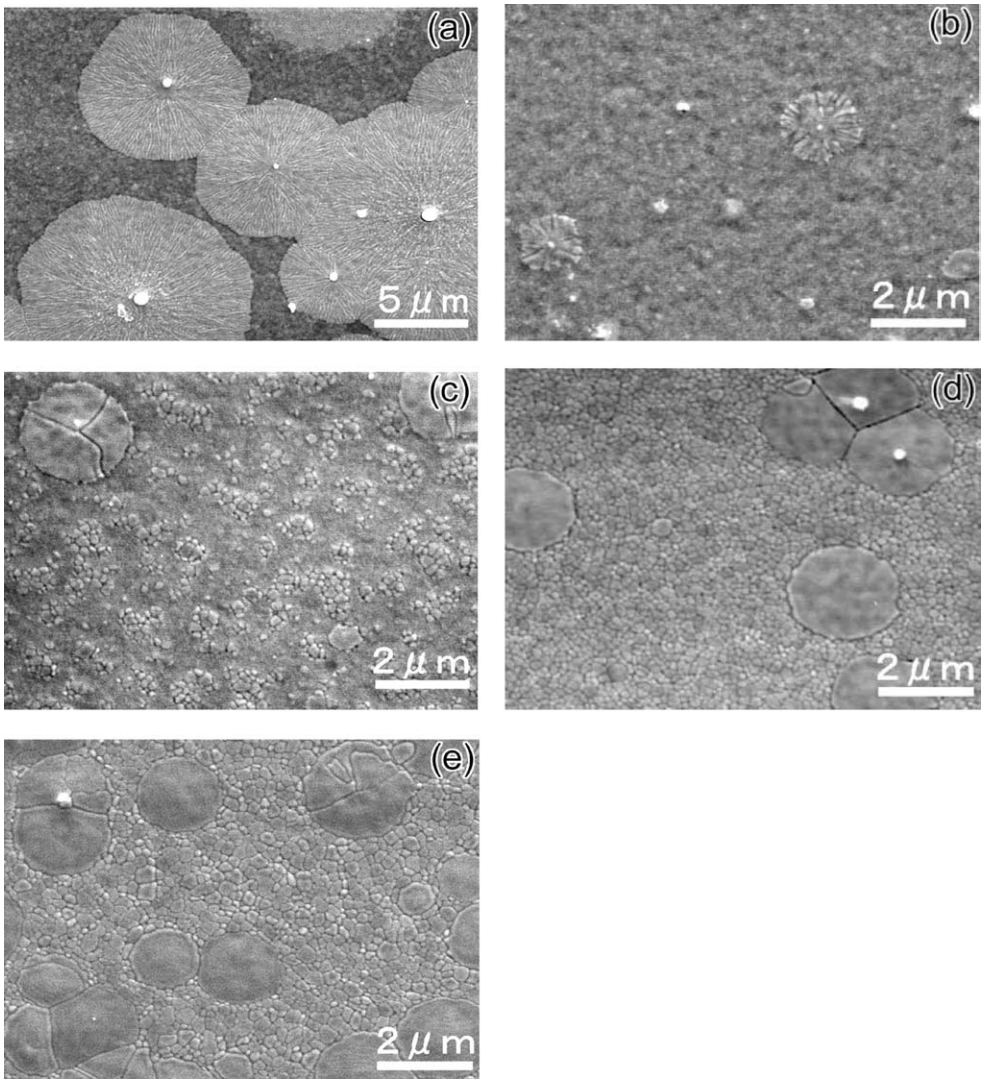

Fig. 3. SEM image of the surface morphology of the PZT films fabricated from targets of $Pb(Zr_xTi_{1-x})O_3$ with Zr/Ti ratios of (a) 70/30, (b) 58/42, (c) 52/48, (d) 45/55 and (e) 30/70.

feature is less conspicuous with increasing titanium composition in the rhombohedral films. The film fabricated from the target with a Zr/Ti ratio of 58/42 showed fine-grained structure in a featureless microstructure except few rosettes with diameter of -2 μm (Fig. 3(b)). In the film fabricated from the target with a Zr/Ti ratio of 52/48, matrix exhibited spherical grain microstructure with grain size ranging from 0.1 to 0.3 μm (Fig. 3(c)). However, the areas of the pyrochlore phase among the spherical grains were still observed. The film did not show rosette structure, but island-like regions with diameters of -2.5 μm were observed. Compositional analysis by energy dispersive spectroscopy (EDS) showed no variation between the island-like regions and the surrounding grains (not shown here), and the island-like regions were identified as the perovskite phase. In the films fabricated from the targets with Zr/Ti ratios of 45/55 and 30/70, no area of the pyrochlore phase among the spherical grains was observed (Fig. 3(d) and (e)). These results reveal a strong influence of Zr/Ti ratios on the microstructure of the PZT films, and the rosette structure and the areas of the pyrochlore phase disappeared with increasing titanium composition.

3.3. *Cross-Sectional Microstructure of the PZT Films*

In the film fabricated from the target with a Zr/Ti ratio of 70/30, large plate-like grains of the rosettes existed at the top of the PZT film, and columnar grains existed at the bottom of the film (Fig. 4(a)). This means that the rosettes only occurred on the surface of the PZT film. The film fabricated from the target with a Zr/Ti ratio of 52/48 showed mainly columnar grains structure. TEM observation showed that some fine-grained pyrochlore phase grains distributed on the top of the film (not shown here). The films fabricated from the target with Zr/Ti ratios of 45/55 and 30/70 had a polycrystalline columnar microstructure extending throughout the thickness of the film except few island-like regions on the top of the film. Figure 4(b) shows the cross-sectional microstructure of the film fabricated from the target with a Zr/Ti ratio of 45/55. In comparison with Fig. 4(a), the width of the columnar grain of the film fabricated from the target with a Zr/Ti ratio of 45/55 is smaller than that of the film fabricated from the target with a Zr/Ti ratio of 70/30. These results indicate that the perovskite grain (occurred from the interface of PZT/Pt) size decrease substantially with increasing Ti concentration of the PZT films, and the rosettes occur in the case of low nucleation density.

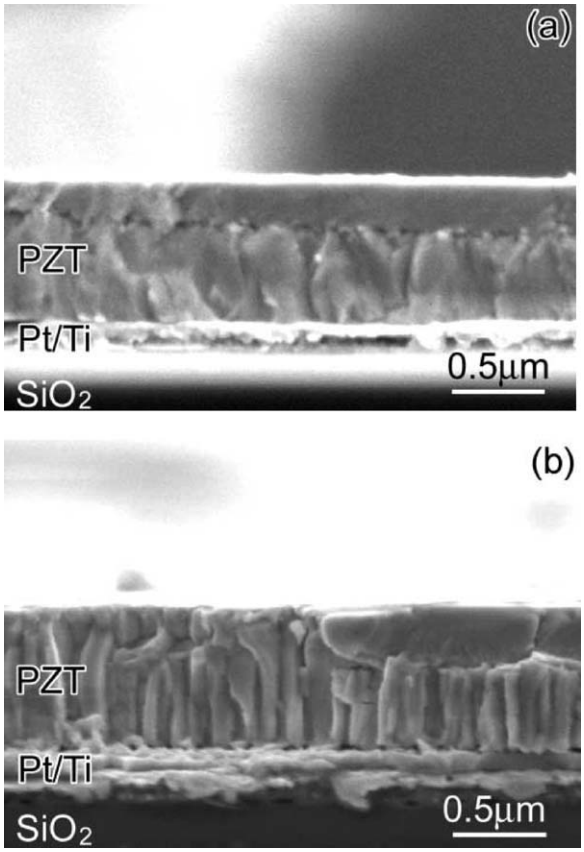

Fig. 4. SEM image of the cross-sectional morphology of the PZT films fabricated from targets of $Pb(Zr_xTi_{1-x})O_3$ with Zr/Ti ratios of (a) 70/30 and (b) 45/55.

3.4. *Electrical Properties of the PZT Films*

The spontaneous polarization, remanent polarization and dielectric constant were shown as a function of Zr/Ti ratio of PZT targets in Fig. 5. The spontaneous polarization, remanent polarization and dielectric constant became larger as the zirconium content decrease in the rhombohedral films, and the PZT films derived from the target with a Zr/Ti ratio of 45/55 has the best electrical properties. The tetragonal film shows a smaller value of the spontaneous polarization, remanent polarization and dielectric constant. It is well known that both dielectric constant and ferroelectricity

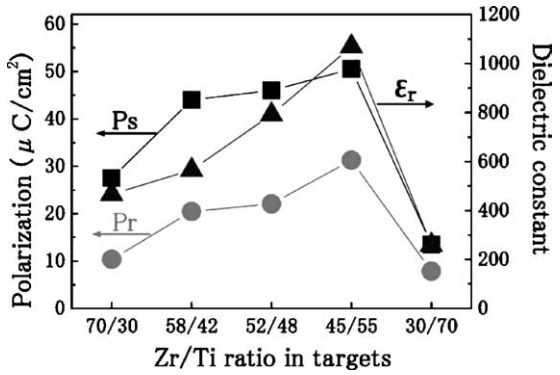

Fig. 5. Average values of the spontaneous polarization (*Ps*), remanent polarization (*Pr*) and Dielectric constant (ε_r) as a function of Zr/Ti ratio in the $Pb(Zr_xTi_{1-x})O_3$ targets.

near MPB are enhanced in PZT bulk ceramic. The PZT film fabricated from the target with a Zr/Ti ratio of 45/55 had the better ferroelectric properties and dielectric constant than that fabricated from the target with a Zr/Ti ratio of 52/48, because its composition was close to MPB composition. In addition, The PZT films derived from the target with a Zr/Ti ratio of 45/55 had a polycrystalline columnar microstructure extending throughout the thickness of the film and no the pyrochlore phase on the surface was observed.

4. Conclusions

$Pb(Zr_xTi_{1-x})O_3$ thin films were prepared by pulsed laser deposition using various targets of $Pb(Zr_xTi_{1-x})O_3$ with Zr/Ti ratios of 70/30, 58/42, 52/48, 45/55 and 30/70 on $Pt/Ti/SiO_2/Si(100)$ substrates. The observation of the microstructure showed that the formation of the pyrochlore phase was inhibited in Ti-rich films, and the film derived from the target with a Zr/Ti ratio of 45/55 had a columnar grain structure and no pyrochlore phase existed on the surface. The films derived from the target with a Zr/Ti ratio of 45/55 exhibited better electric properties than that derived from the target with a Zr/Ti ratio of 52/48.

References

1. J. Chu, Z.J. Wang, and R. Maeda, *Jpn. J. Appl. Phys.*, **38**L, 1482 (1999).
2. J. Chu, Z. Wang, R. Maeda, K. Kataoka, T. Itoh, and T. Suga, *J. Vac. Sci. Technol.*, **B18**, 3604 (2000).
3. J. Tsaur, Z.J. Wang, L. Zhang, M. Ichiki, J.W. Wan, and R. Maeda, *Jpn. J. Appl. Phys.*, **41**, 6664 (2002).
4. J. Tsaur, Z.J. Wang, L. Zhang, M. Ichiki, R. Maeda, and Suga, *Proceedings of SPIE*, **4936**, 215 (2002).
5. R. Maeda, Z.J. Wang, J. Chu, J. Akedo, M. Ichiki, and S. Yonekubo, *Jpn. J. Appl. Phys.*, **37**, 7116 (1998).
6. G. Yi, Z. Wu, and M. Sayer, *J. Appl. Phys.*, **64**, 2717 (1988).
7. Z.J. Wang, K. Kikuchi, and R. Maeda, *Jpn. J. Appl. Phys.*, **39**, 5413 (2000).
8. Y. Fukuda and K. Aoki, *Jpn. J. Appl. Phys.*, **36**, 5793 (1997).
9. B. Jaffe, W.R. Cook, and H. Jaffe, *Piezoelectric Ceramics* (Academic Press, London, 1971), p. 142.
10. Z.J. Wang, I. Karibe, L.J. Yan, H. Kokawa, and R. Maeda, *Jpn. J. Appl. Phys.*, **41**, 6658 (2002).
11. Z.J. Wang, I. Karibe, R. Maeda, and H. Kokawa, *J. Am. Ceram. Soc.*, **85**, 3108 (2002).
12. S.A. Myers and L.N. Chapin, *Mat. Res. Soc. Symp. Proc.*, **200**, 231 (1990).
13. A. Carim, B.A. Tuttle, D.H. Doughty, and S.L. Martinez, *J. Am. Ceram. Soc.*, **74**, 1455 (1991).
14. C.K. Kwok and S.B. Desu, *Appl. Phys. Lett.*, **60**, 1430 (1992).
15. Z.J. Wang, R. Maeda, M. Ichiki, and H. Kokawa, *Jpn. J. Appl. Phys.*, **40**, 5523 (2001).